

THE UNIVERSITY OF MICHIGAN

COLLEGE OF ENGINEERING

Department of Engineering Mechanics

Department of Mechanical Engineering

Tire and Suspension Systems Research Group

Technical Report No. 20

THE DYNAMIC STIFFNESS OF A PNEUMATIC TIRE MODEL

R. N. Dodge

S. K. Clark

B. Vahidi

administered through:

OFFICE OF RESEARCH ADMINISTRATION ANN ARBOR

March 1965

⇒ 871

UMR0653

The Tire and Suspension Systems Research Group
at The University of Michigan is sponsored by:

FIRESTONE TIRE AND RUBBER COMPANY

GENERAL TIRE AND RUBBER COMPANY

B. F. GOODRICH TIRE COMPANY

GOODYEAR TIRE AND RUBBER COMPANY

UNITED STATES RUBBER COMPANY

TABLE OF CONTENTS

	Page
LIST OF FIGURES	vii
NOMENCLATURE	ix
I. ABSTRACT	1
II. FOREWORD	3
III. ANALYSIS OF A ROTATING CYLINDRICAL SHELL SUPPORTED BY AN ELASTIC FOUNDATION	5
IV. POINT LOAD PROBLEM	9
V. EXPERIMENTAL MEASUREMENTS	17
ACKNOWLEDGMENT	26
REFERENCES	27
DISTRIBUTION LIST	29

LIST OF FIGURES

FIGURE	Page
1. Basic cylindrical shell model for a pneumatic tire.	6
2. Coordinate nomenclature.	6
3. Externally applied point-load to shell model.	9
4. Experimental test model.	17
5. Schematic of test stand.	19
6. Load vs deflection. Test model 1. $\Omega = 0$	21
7. Load vs deflection. Test model 1. $\Omega = 400$ rpm.	22
8. Load vs deflection. Test model 1. $\Omega = 800$ rpm.	23
9. Load vs deflection. Test model 1. $\Omega = 1200$ rpm.	24
10. Load vs deflection. Test model 1. $\Omega = 1600$ rpm.	25

NOMENCLATURE

ENGLISH LETTERS

a_0	-	Undeformed radius of cylindrical shell, measured to the midline of shell thickness
a, b	-	Real and imaginary parts of roots
b_w	-	Width of cylindrical shell. This would normally correspond approximately to tread width
C	-	Constants of integration
E	-	Young's modulus of shell material
e	-	Base of natural logarithms
h	-	Shell thickness
i	-	$\sqrt{-1}$
k	-	Elastic stiffness of shell internal foundation
\bar{k}	-	$k a_0^2 / Eh$
p	-	Inflation pressure
p^*	-	$6a_0^2 p / b_w Eh^3$
r	-	Radius or radial dimension
t	-	Time
v, w	-	Shell displacement in tangential and radial direction, respectively.
X_1, X_2	-	Fixed co-ordinate directions
x_1, x_2	-	Rotating co-ordinate directions
z	-	w/a_0 , a dimensionless variable

NOMENCLATURE (Concluded)

GREEK LETTERS

α^2	-	$h^2/12a_0^2$, a dimensionless constant
ρ	-	Shell material density
Ω	-	Shell angular velocity
θ	-	Angular co-ordinate
θ_1	-	$\theta - \Omega t$
ψ	-	v/a_0 , a dimensionless variable
$\bar{\omega}^2$	-	$\frac{\Omega^2 a_0^2 \rho}{E}$, a dimensionless variable

I. ABSTRACT

The problem of the rotating cylindrical shell under the action of a stationary point load is treated in detail as a means of approximating the action of a tire while rolling. Comparison is made between calculated and measured load deflection curves using a model very similar to the postulated cylindrical shell. There is reasonable correlation between such dynamic load deflection characteristics as predicted from the model and obtained experimentally, so that some support is lent to the eventual application of this model as an analog for real pneumatic tire studies.

II. FOREWORD

This paper utilizes a rotating cylindrical shell as a model by which one may approximate the dynamic response of a real pneumatic tire. This circular cylindrical shell is presumed to have characteristics such as shown in Figure 1, where a relatively inextensible outer band of known elastic properties is supported by an elastic foundation which in turn is caused to rotate about a central hub. The width of this shell is considered small compared to its diameter or radius.

There are two reasons for studying the response of such a shell to a stationary point load. The first is that such a model may be quite easily constructed from conventional materials whose properties are well known, so that experiments may be carried out to compare the actual deflection under point load of such a model with calculations made using the expressions developed analytically for this problem. This allows correlation between theory and experiment in a much more secure way than could be accomplished using a real pneumatic tire. The real pneumatic tire suffers from the disadvantage of having very complex and variable elastic properties, as well as having a geometry which is not immediately susceptible to interpretation in terms of cylindrical shell dimensional parameters.

The second reason for studying such a problem is that it represents an approximation to a real pneumatic tire running under fairly light contact loads. The analytical solution of this problem, representing the light

contact loads by an idealized point load, is rather straight forward and allows a fairly complete analytical solution to be obtained for this problem. Thus, one may study this problem analytically in a more thorough way than the more complicated problems involving finite contact area between the tire and the roadway. Details of the motion outside the contact patch may thus be examined in considerably more detail here than in other solutions. Thus, one of the primary aims of this paper is to discuss motion outside the contact patch while the tire is rolling.

The specific problem treated here is that of determining expressions for the load deflection characteristics of a rotating cylindrical shell loaded by an external stationary point load. Both analytical and experimental calculations are presented for a single model.

III. ANALYSIS OF A ROTATING CYLINDRICAL SHELL
SUPPORTED BY AN ELASTIC FOUNDATION

It has been pointed out in References 1 and 2 that some hope exists that the dynamic properties of the pneumatic tire may be well described by the same set of equations that describes the motion of a circular cylindrical shell. One must consider the circular cylindrical shell to be internally supported by an elastic foundation such as is illustrated in Figure 1. In this case, no loss mechanism will be assumed in the generalized foundation so that its response is purely elastic.

In Figure 2 the coordinate system is shown defining the displacements associated with the circular cylindrical shell. A stationary coordinate system X_1, X_2 is fixed in space. Rotating about this origin with the rotating shell is a moving coordinate system x_1, x_2 , while attached to the shell itself are the coordinates for displacement w, v in the radial and tangential directions respectively. Equation (1) defines certain variables which are used:

$$\begin{aligned} r &= a_0 + w \\ z &= \frac{w}{a_0} \\ \psi &= \frac{v}{a_0} \\ \alpha^2 &= \frac{h^2}{12a_0^2} \\ t &= \text{time} \end{aligned} \tag{1}$$

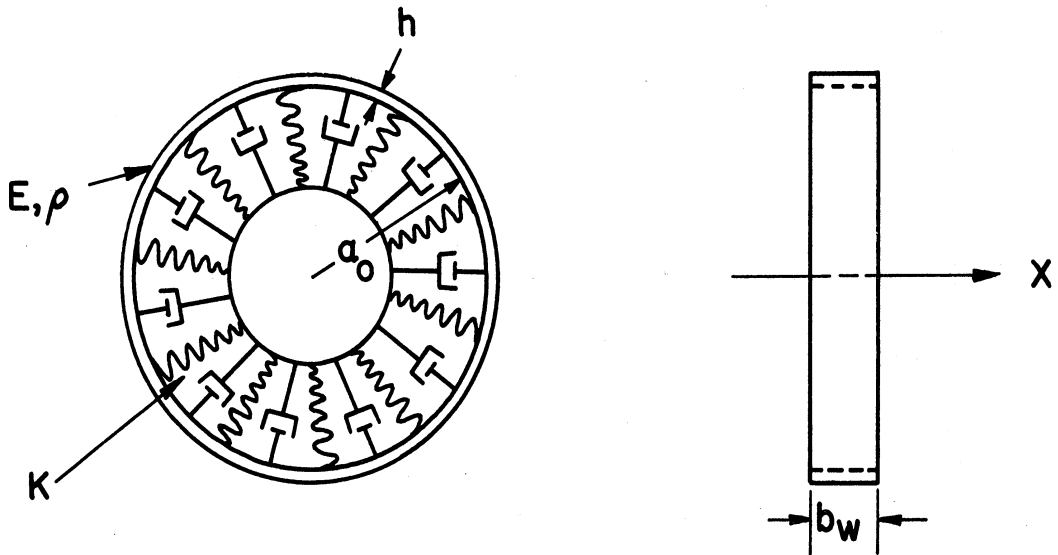


Figure 1. Basic cylindrical shell model for a pneumatic tire.

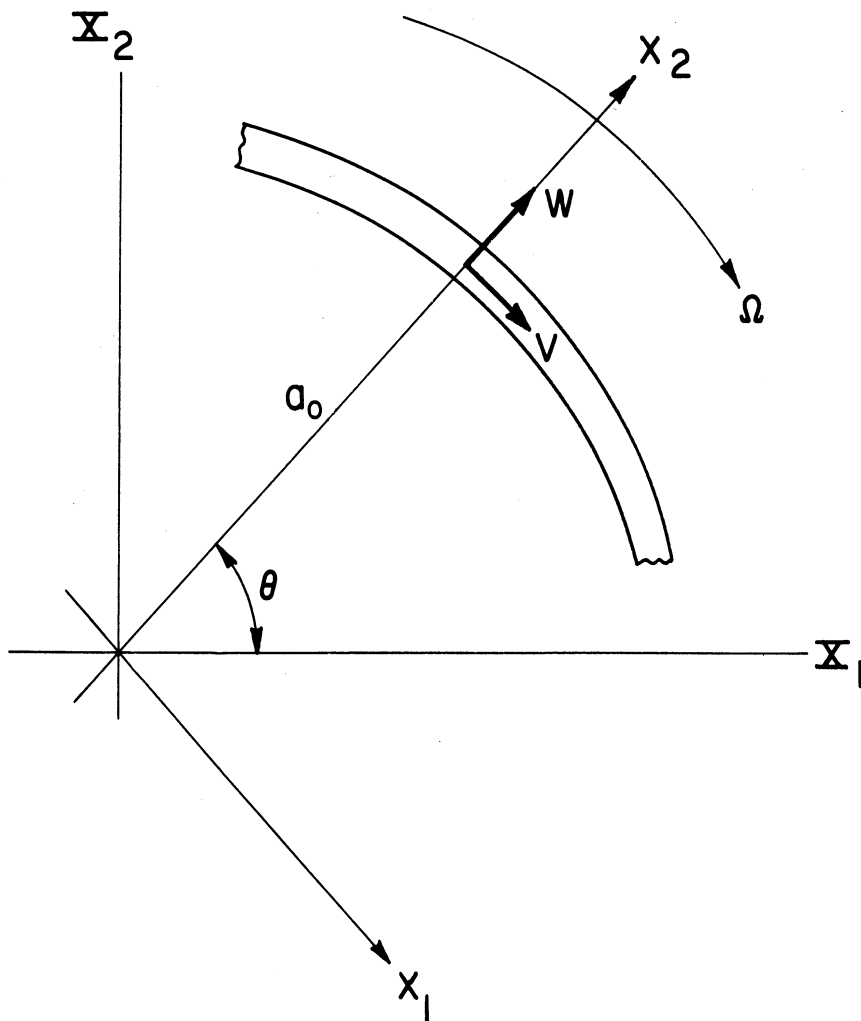


Figure 2. Coordinate nomenclature.

Note that the angle Θ is measured relative to the moving coordinate system x_i . As has been shown in Reference 1, the equations of motion, in terms of the moving coordinates of such a shell, are:

$$\ddot{z} - \Omega(2\dot{\psi} + \Omega z + \dot{\Omega}) + \frac{Eh^2}{12\rho a_0^4} (z^{IV} + 2z'' + z) + \frac{E}{\rho a_0^2} (\psi' + z) + \frac{E}{\rho} \left(\frac{kz}{Eh} \right) = 0 \quad (2)$$

$$\ddot{\psi} - \Omega(\Omega\psi - 2\dot{z}) - \frac{E}{\rho a_0^2} (\psi'' + z') = 0$$

The primes and dots denote differentiation with respect to Θ and t , respectively.

The development of Eqs. (2) is predicated upon the following assumptions:

- (a) Plane strain is assumed; i.e., the strain parallel to the generators of the shell is everywhere zero.
- (b) Relative motion is assumed small enough so that products of displacements and their derivatives can be neglected with respect to first order terms. This implies that Eqs. (2) are the linearized form of the equations of motion.
- (c) This development considers only those effects due to the deformation of the supporting elastic foundation, the deformation due to rotational effects, and local deformations due to bending. Damping has not been included.
- (d) Lateral contraction of the shell parallel to the generators has been neglected for convenience.

In Eqs. (2), k represents the local spring constant per unit area of the supporting elastic foundation, ρ is the mass density of the shell band, E is the extension modulus of the shell band, and Ω is the constant angular velocity of the combined shell and its supporting foundation.

IV. POINT LOAD PROBLEM

The point-load geometry is illustrated in Figure 3. There, it is seen that a concentrated load P is applied to the model at a fixed point in

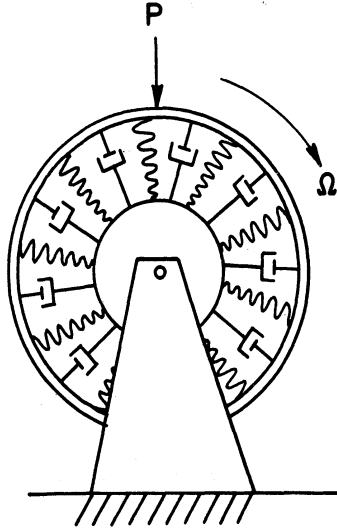


Figure 3. Externally applied point-load to shell model.

space. In order to cause this point in space to remain fixed, it is convenient to introduce the new coordinates:

$$t_1 = t, \quad \theta_1 = \theta + \Omega t \quad (3)$$

By use of such coordinates, it may be seen that the load P may be applied at the point $\theta_1 = 0$, which now corresponds to a fixed point in space.

Equations (2) may be expressed in terms of these new coordinates. Omitting the details of such a transformation, one obtains from Eqs. (2):

$$\ddot{z} + 2\Omega\dot{z}' + \Omega^2 z'' - \Omega[2(\dot{\psi} + \Omega\psi') + \Omega z + \Omega] + \frac{Eh^2}{12\rho a_0^4} (z^{IV} + 2z'' + z) + \frac{E}{\rho a_0^2} (\psi' + z) + \frac{E}{\rho} \left(\frac{kz}{Eh}\right) = 0 \quad (4)$$

$$\ddot{\psi} + 2\Omega\dot{\psi}' + \Omega^2 \psi'' - \Omega[\Omega\psi - 2(\dot{z} + \Omega z')] - \frac{E}{\rho a_0^2} (\psi'' + z') = 0$$

where dots and primes now indicate differentiation with respect to t_1 and Θ_1 , respectively.

We are interested here in steady state running conditions, in which case the transient terms of Eqs. (4) vanish since they represent transients with respect to our Θ_1 - t_1 coordinate system, a system which is now fixed in space. The omission of time dependent terms of Eqs. (4) results in a steady state equation which describes the geometry of the standing waves in the rotating shell with respect to the Θ_1 , or fixed, coordinate system. Such equations become

$$z^{IV} + \left(2 + \frac{\bar{\omega}^2}{\alpha^2}\right)z'' + \left(1 + \frac{\bar{k}}{\alpha^2} + \frac{1}{\alpha^2} - \frac{\bar{\omega}^2}{\alpha^2}\right)z + \left(\frac{1}{\alpha^2} - \frac{2\bar{\omega}^2}{\alpha^2}\right)\psi' = \frac{\bar{\omega}}{\alpha^2}$$

$$\left(\frac{\bar{\omega}^2}{\alpha^2} - \frac{1}{\alpha^2}\right)\psi'' - \frac{\bar{\omega}^2}{\alpha^2}\psi - \left(\frac{1}{\alpha^2} - \frac{2\bar{\omega}^2}{\alpha^2}\right)z' = 0 \quad (5)$$

where

$$\bar{\omega}^2 = \frac{\Omega^2 a_0^2 \rho}{E}, \quad \bar{k} = \frac{ka_0^2}{Eh}$$

In view of the fact that the coefficients of z and its derivatives are con-

stant for constant Ω , ρ , h , a_0 and E , then Eqs. (5) take the form:

$$\begin{aligned} z^{IV} + A_1 z'' + A_2 z + A_3 \psi' &= A_4 \\ A_5 \psi'' - A_4 \psi - A_3 z' &= 0 \end{aligned} \quad (5a)$$

The quantity ψ may be eliminated from Eqs. (5a) yielding a single sixth order differential equation in the radial dimensionless displacement z .

$$z^{VI} + H_1 z^{IV} + H_2 z'' - H_3 z = -H_4 \quad (6)$$

where

$$\begin{aligned} H_1 &= \frac{\bar{\omega}^2}{\alpha^2} \left[1 - \frac{\alpha^2}{(\bar{\omega}^2 - 1)} \right] + 2 \\ H_2 &= 1 + \frac{\bar{k}}{\alpha^2} + \frac{1}{\alpha^2} - \frac{\bar{\omega}^2}{\alpha^2} \left[1 + \frac{(2\alpha^2 + \bar{\omega}^2)}{(\bar{\omega}^2 - 1)} \right] + \frac{(1 - 2\bar{\omega}^2)^2}{\alpha^2 (\bar{\omega}^2 - 1)} \\ H_3 &= \frac{\bar{\omega}^2}{(\bar{\omega}^2 - 1)} \left[1 + \frac{\bar{k}}{\alpha^2} + \frac{1}{\alpha^2} - \frac{\bar{\omega}^2}{\alpha^2} \right] \\ H_4 &= \frac{(\bar{\omega}^2)^2}{\alpha^2 (\bar{\omega}^2 - 1)} \end{aligned} \quad (7)$$

A particular solution of Eq. (6) is:

$$z_p = \frac{-H_4}{-H_3} = \frac{\bar{\omega}^2}{\alpha^2} / \left(1 + \frac{\bar{k}}{\alpha^2} + \frac{1}{\alpha^2} - \frac{\bar{\omega}^2}{\alpha^2} \right) \quad (8)$$

If the solution to the homogeneous equation formed from Eq. (6) is assumed to be of the type $z_c = Ae^{q\theta_1}$, then the characteristic equation for q is:

$$q^6 + H_1 q^4 + H_2 q^2 - H_3 = 0 \quad (9)$$

This may be rewritten as

$$Q^3 + H_1 Q^2 + H_2 Q - H_3 = 0 \quad (10)$$

where $Q = q^2$.

Upon consideration of the form of H_1 , H_2 and H_3 , it may be shown that the solutions of Eq. (10) consist of one negative root (Q_1) and a pair of complex conjugate roots (Q_2 and Q_3). The root Q_1 leads to pure imaginary q , while Q_2 and Q_3 lead to a pair of complex conjugate q 's. These roots are represented as:

$$q_{1-2} = \pm i b_1 \text{ from } Q_1$$

$$q_{3-4} = \pm (a_2 + i b_2) \text{ from } Q_2$$

$$q_{5-6} = \pm (a_2 - i b_2) \text{ from } Q_3$$

Thus the homogeneous solution of Eq. (6) is

$$z_c = C_1 \cos b_1 \theta_1 + C_2 \sin b_1 \theta_1 + e^{a_2 \theta_1} [C_3 \cos b_2 \theta_1 + C_4 \sin b_2 \theta_1] + e^{-a_2 \theta_1} [C_5 \cos b_2 \theta_1 + C_6 \sin b_2 \theta_1] \quad (11)$$

It is instructive to view Eq. (11) first from the point of view of angles θ_1 lying between 0 and π . In this region of positive angle, one physically expects the effects of the point load to be relatively small at the upper surface of the shell denoted by $\theta_1 = \pi$. This leads immediately to the realization that the constants C_3 and C_4 of Eq. (11) must be quite small. Further, if we restrict attention primarily to the region θ_1 small, then

the effect of the small constants C_3 and C_4 upon the overall solution must be nearly negligible. By such a line of reasoning, one may separate out Eq. (11) into two portions, one valid for positive angles, or forward of the point of load application, while the second portion is valid aft of the point of load application, say in the region θ_1 up to $-\pi$. This is expressed analytically in Eqs. (12).

$$z_1 = C_1 \cos b_1 \theta_1 + C_2 \sin b_1 \theta_1 + e^{-a_2 \theta_1} [C_5 \cos b_2 \theta_1 + C_6 \sin b_2 \theta_1]$$

$$\text{For } 0 < \theta_1 < \pi$$

(12)

$$z_2 = C_1 \cos b_1 \theta_1 + C_2 \sin b_1 \theta_1 + e^{a_2 \theta_1} [C_3 \cos b_2 \theta_1 + C_4 \sin b_2 \theta_1]$$

$$\text{For } -\pi < \theta_1 < 0$$

The constants appearing in Eqs. (12) may be evaluated using equations expressing the continuity of the dimensionless deflection and its derivatives across the load point, as well as the continuity of such quantities at the upper edge of the shell. These are given in Eqs. (13).

$$z_1(\theta_1 = 0^+) - z_2(\theta_1 = 0^-) = 0 \quad (a)$$

$$z_1'(\theta_1 = 0^+) - z_2'(\theta_1 = 0^-) = 0 \quad (b)$$

$$z_1''(\theta_1 = 0^+) - z_2''(\theta_1 = 0^-) = 0 \quad (c)$$

$$z_1'''(\theta_1 = 0^+) - z_2'''(\theta_1 = 0^-) = 2P^* \quad (d)$$

$$z_1(+\pi^-) - z_2(-\pi^+) = 0 \quad (e)$$

(13)

$$z_1'(+\pi^-) - z_2'(-\pi^+) = 0 \quad (f)$$

where

$$P^* = \frac{6a_0^2 P}{b_w \cdot E h^3}$$

Note that Eq. (13a) represents continuity of displacement at $\theta_1 = 0$, Eq. (13b) represents continuity of slope, Eq. (13c) continuity of bending moment and Eq. (13d) indicates that the sum of the shear forces is equal to the total applied force P . Equations (13e) and (13f) represent continuity of displacement and slope at the point $\theta_1 = \pi$ or $-\pi$. Using these conditions, along with the solutions of Eqs. (12), the constants C_3 , C_4 , C_5 and C_6 are found to be:

$$\begin{aligned} C_3 = C_5 &= \frac{P^*}{2a_2(b_2^2 + a_2^2)} \\ C_6 = -C_4 &= \frac{P^*}{2b_2(b_2^2 + a_2^2)} \end{aligned} \tag{14}$$

and from (13e) and (13f)

$$\begin{aligned} C_2 &= 0 \\ C_1 &= \frac{e^{-a_2 \pi} [\sin(b_2 \pi)] P^*}{-2b_1 a_2 b_2 \sin(b_1 \pi)} \end{aligned}$$

Combining Eqs. (8), (12) and (14) gives finally solutions for the dimensionless deformation z due to a point-load applied at $\theta_1 = 0$ in the form

$$z_1 = \frac{p^*}{2} \left\{ \frac{e^{-a_2 \pi} [\sin(b_2 \pi)] \cos b_1 \theta_1}{-b_1 a_2 b_2 \sin(b_1 \pi)} + \frac{e^{-a_2 \theta_1}}{(b_2^2 + a_2^2)} \left[\frac{1}{a_2} \cos b_2 \theta_1 + \frac{1}{b_2} \sin b_2 \theta_1 \right] \right\} + \frac{\omega^2}{\alpha^2} / \left(1 + \frac{k}{\alpha^2} + \frac{1}{\alpha^2} - \frac{\omega^2}{\alpha^2} \right) \quad \underline{0 < \theta_1 < \pi} \quad (15)$$

$$z_2 = \frac{p^*}{2} \left\{ \frac{e^{-a_2 \pi} [\sin(b_2 \pi)] \cos b_1 \theta_1}{-b_1 a_2 b_2 \sin(b_1 \pi)} + \frac{e^{a_2 \theta_1}}{(b_2^2 + a_2^2)} \left[\frac{1}{a_2} \cos b_2 \theta_1 - \frac{1}{b_2} \sin b_2 \theta_1 \right] \right\} + \frac{\omega^2}{\alpha^2} / \left(1 + \frac{k}{\alpha^2} + \frac{1}{\alpha^2} - \frac{\omega^2}{\alpha^2} \right) \quad \underline{-\pi < \theta_1 < 0}$$

Note that it is rather difficult to interpret the influence of any single parameter upon the load deflection relationships as given by Eq. (15), since almost all of the quantities entering into these relationships are derived from the cubic Eq. (10) whose solutions are difficult to estimate in terms of the input parameters. However, the calculations which have been done seem to indicate the following results, given with the restriction that they may not represent general conclusions but are rather specific conclusions for the model used later on in the experimental studies:

- (a) At a given value of load P^* , the deflection z at the point $\theta_1 = 0$ increases slightly as speed increases since the quantity a_2 in the denominator decreases more rapidly than the quantity $(a_2^2 + b_2^2)$ increases.
- (b) The first term of Eq. (15) represents an undamped harmonic wave which travels completely around the circumference of the shell. The magnitude of this wave starts with a negative value, but increases with speed so that it moves closer toward zero. It would be expected that at high speeds this magnitude would pass through zero and become a larger positive number.

- (c) The second term of Eqs. (15) represents a damped harmonic wave with maximum amplitude at the point of load application. The damping constant a_2 decreases as the angular velocity increases so that the wave becomes more pronounced around a greater portion of the circumference of the shell.
- (d) It will be recognized that identical conclusions hold for the second of Eqs. (15) as for the first.

V. EXPERIMENTAL MEASUREMENTS

A model designed to provide a means of conducting simple experiments verifying the applicability of Eqs. (15) was built, and is illustrated in Figure 4 where the model elastic constants are $k = 27 \text{ lb/in.}^3$, $Eh^3 = 55 \text{ lb-in.}$, $\alpha^2 = 3.121 \times 10^{-5}$, $a_0 = 3.875 \text{ in.}$, and $\rho h = 1.51 \times 10^{-5} \text{ slug-ft./in.}^3$. The cylindrical shell used here is made of a thin rubber belt reinforced with twisted steel cords wrapped in the circumferential direction, and is merely the core of an ordinary timing belt. The elastic foundation consists of a sponge rubber insert bonded to the belt with silicone rubber. This elastic foundation is attached to a central hub of plexiglass and aluminum.

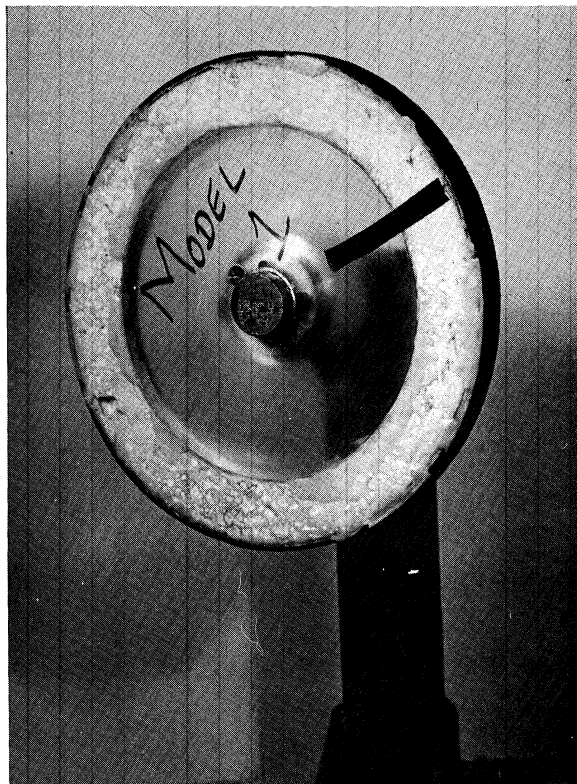


Figure 4. Experimental test model.

Table I gives load deflection data taken on the model in a stationary position and under a point load at $\theta_1 = 0$. The test stand used for these experiments is illustrated in Figure 5. It consists of a variable speed motor for controlling the angular velocity, a pivoted arm for applying the load, a ball bearing roller to serve as the loading point, and a load cell for measuring magnitude of the applied load. A mechanical dial gauge records the deflection of this load.

TABLE I

POINT LOAD VS. DEFLECTION AT $\Omega = 400$ RPM

Load, lb	Deflection, in.
0	0
-1.	-.021
-2.	-.041
-3.	-.061
-4.	-.079
-5.	-.095
-6.	-.119
-7.	-.145
-8.	-.171
-9.	-.198

In collecting this data the deflection measurements were made after the model was running at its prescribed angular velocity. This introduces a slight error when such measurements are compared with calculations done on the basis of Eqs. (15), since these do not include the deformation due to pure rotational effects. However, as can be seen from the calculations, the deformation due to these effects was very small compared with the bending

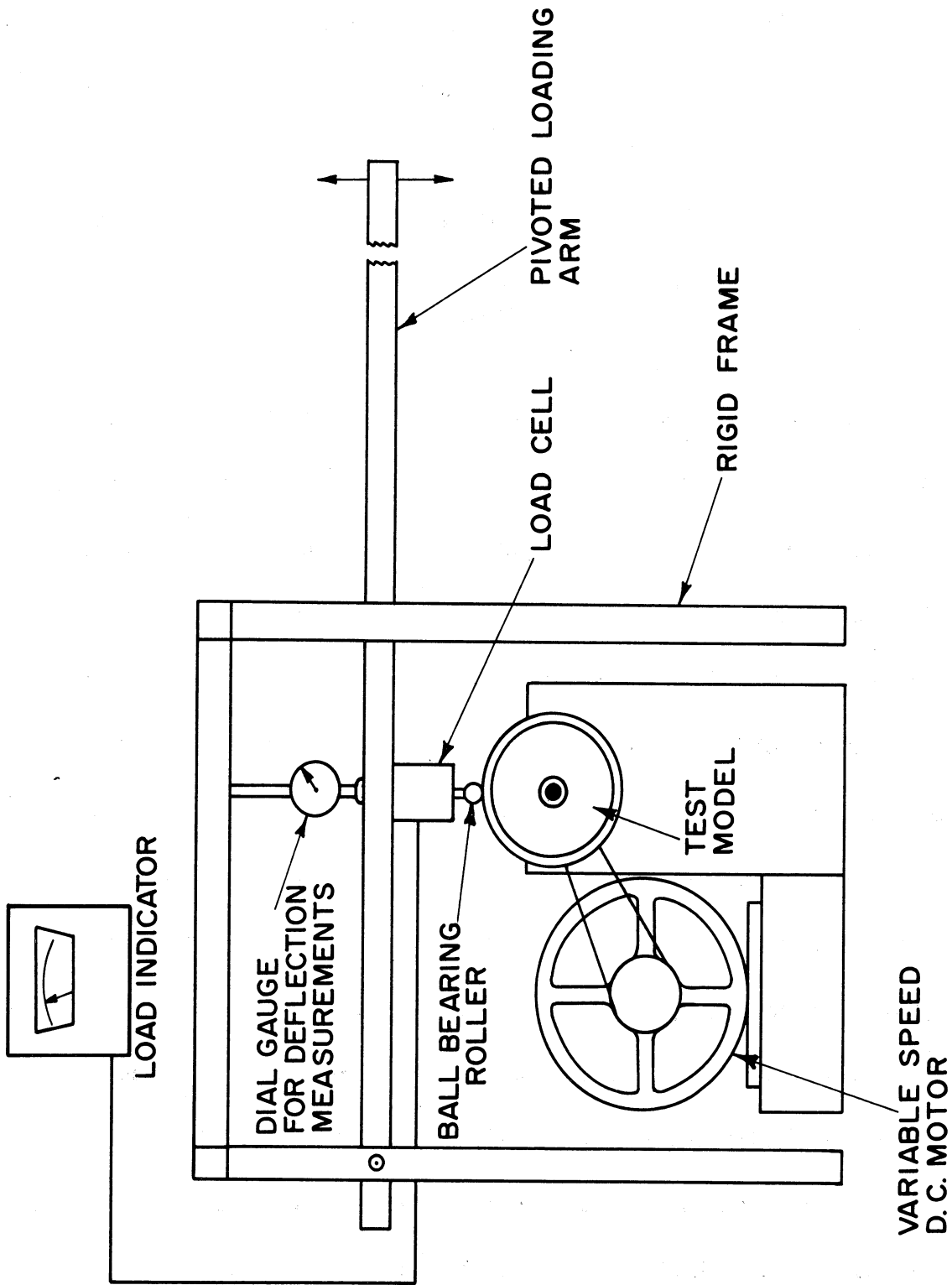


Figure 5. Schematic of test stand.

deformation. An additional error was introduced since the roller representing the point load was a finite radius of curvature. This causes the contact to be over some length, a situation not contemplated in the analytical solution given by Eq. (15). However, comparison between static load-deflection data taken with the model loaded against a sharp edge and loaded against the roller used here seems to indicate that the differences between the two load-deflection relations should be negligible.

Typical load-deflection data taken from the rotating shell model are shown in Figures 6-10. Load deflection curves predicted from Eqs. (15) are also given for these same tests as solid lines on the figures. Note that, in general, agreement seems to be reasonably good since the elastic data for the model were obtained by separate measurements of its components before assembly. Calculations made on the basis of Eqs. (15) seem to be somewhat less successful at higher rotating speeds, and further work on these dynamic effects is probably necessary.

In general, one would expect the deflection of such a system to increase with speed under a constant load since, as has been pointed out by Kenney in Reference 4, by increasing surface speed one is moving up the left hand branch of a simple resonance diagram corresponding to the equality of surface speed with the wave propagation velocity for bending disturbances. That particular resonant condition should result, in the undamped case, in indefinitely large deflections per unit load so that in general the deflections should be increasing.

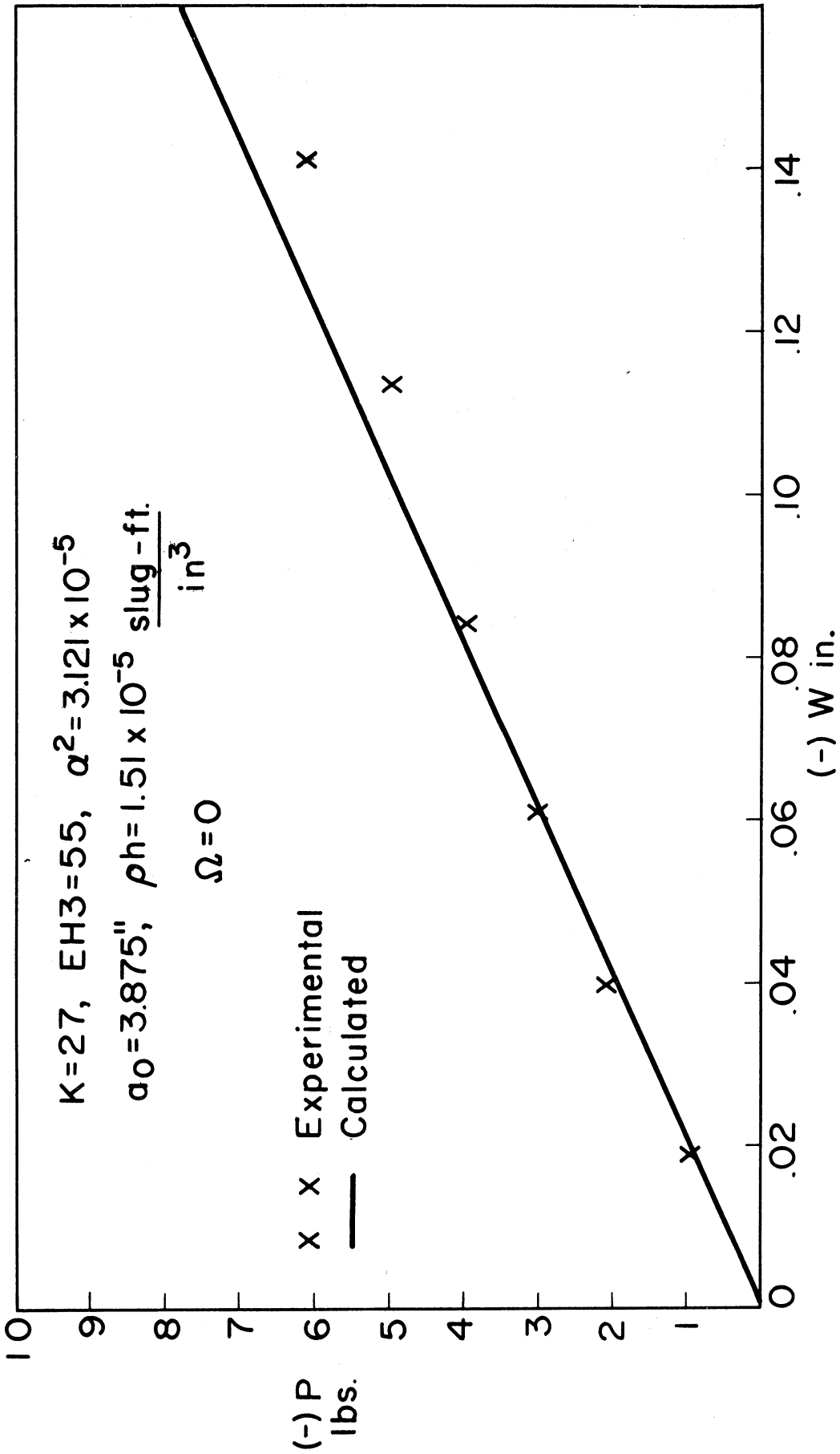


Figure 6. Load vs deflection. Test model 1. $\Omega = 0$

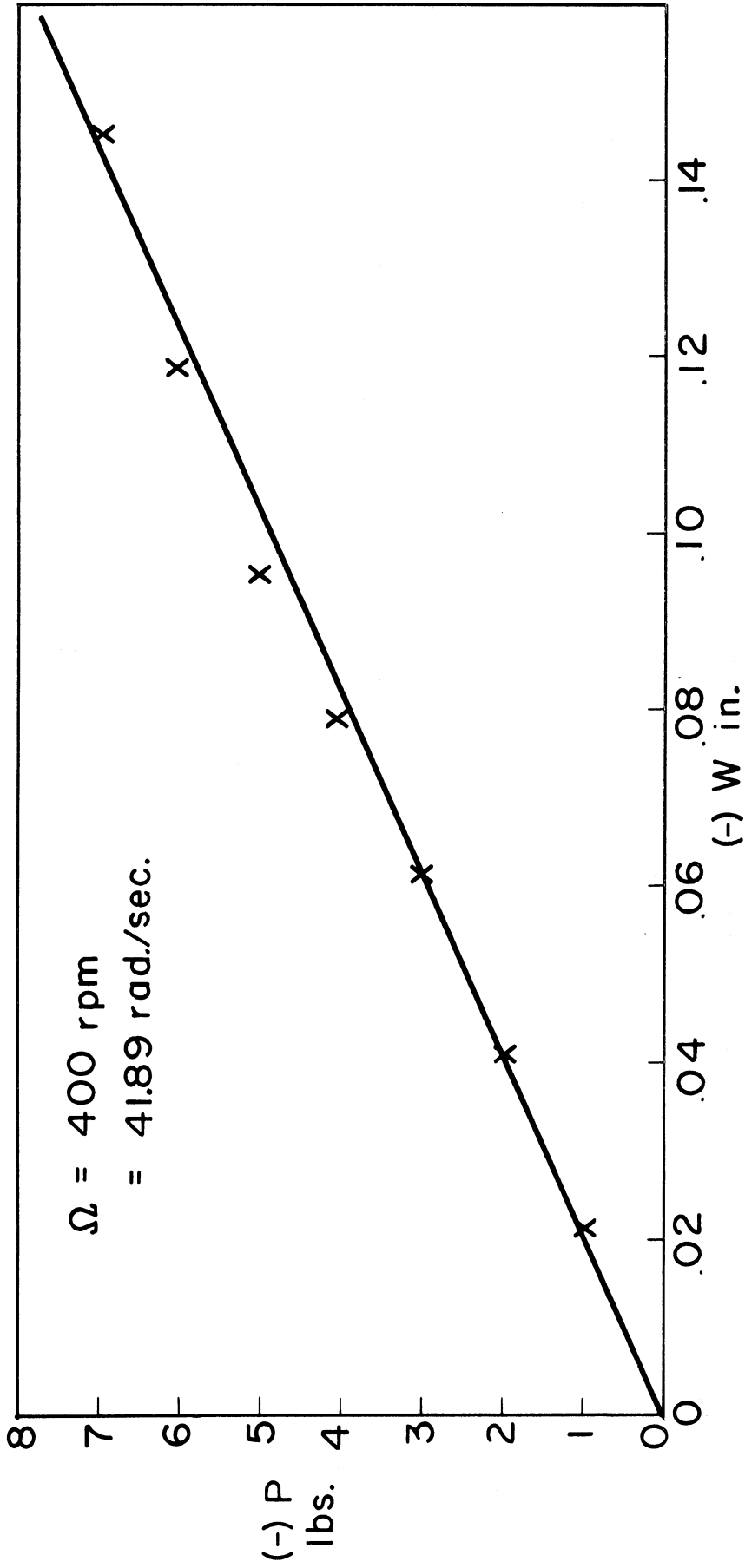


Figure 7. Load vs deflection. Test model I. $\Omega = 400 \text{ rpm.}$

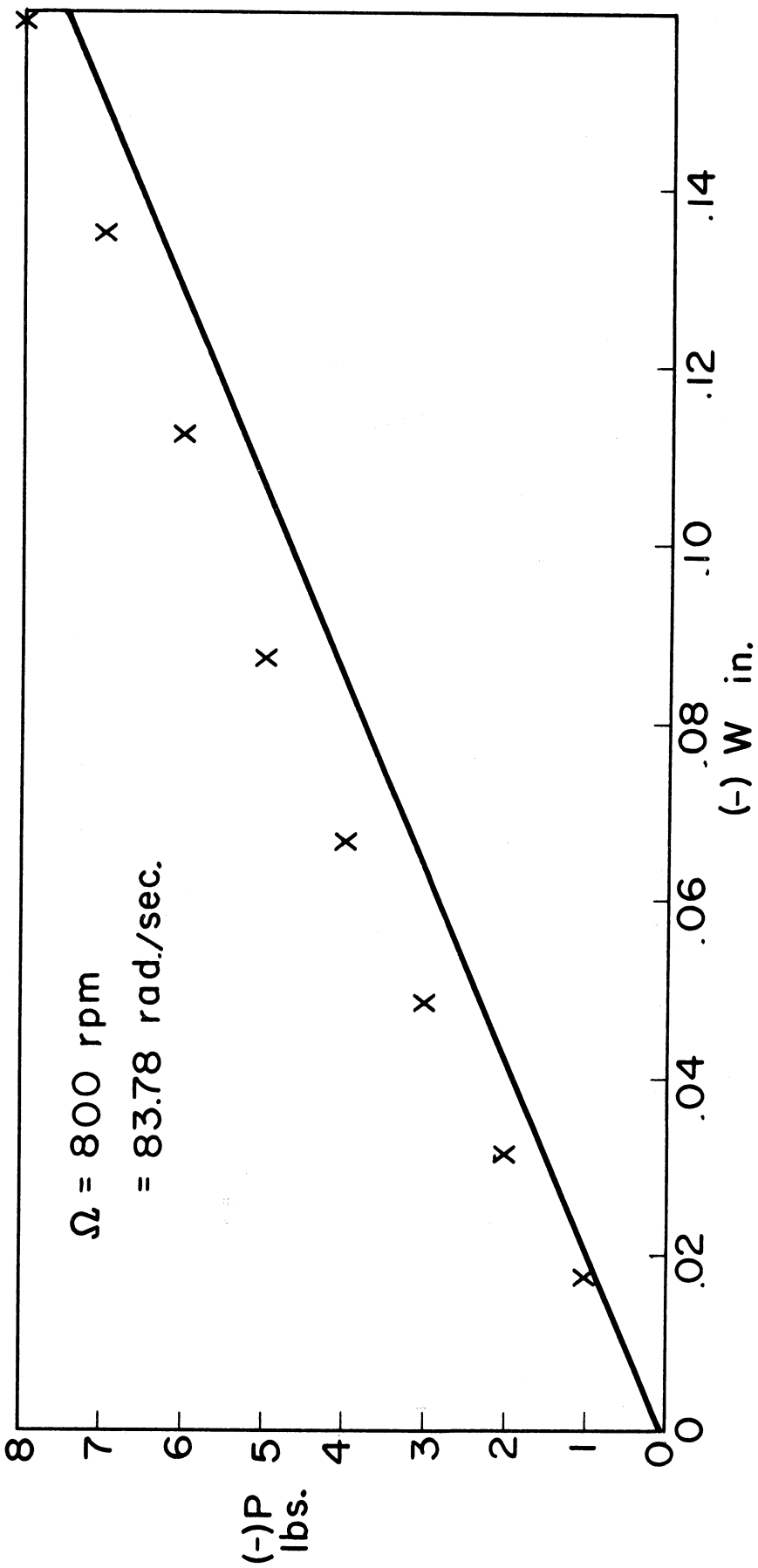


Figure 8. Load vs deflection. Test model 1. $\Omega = 800 \text{ rpm.}$

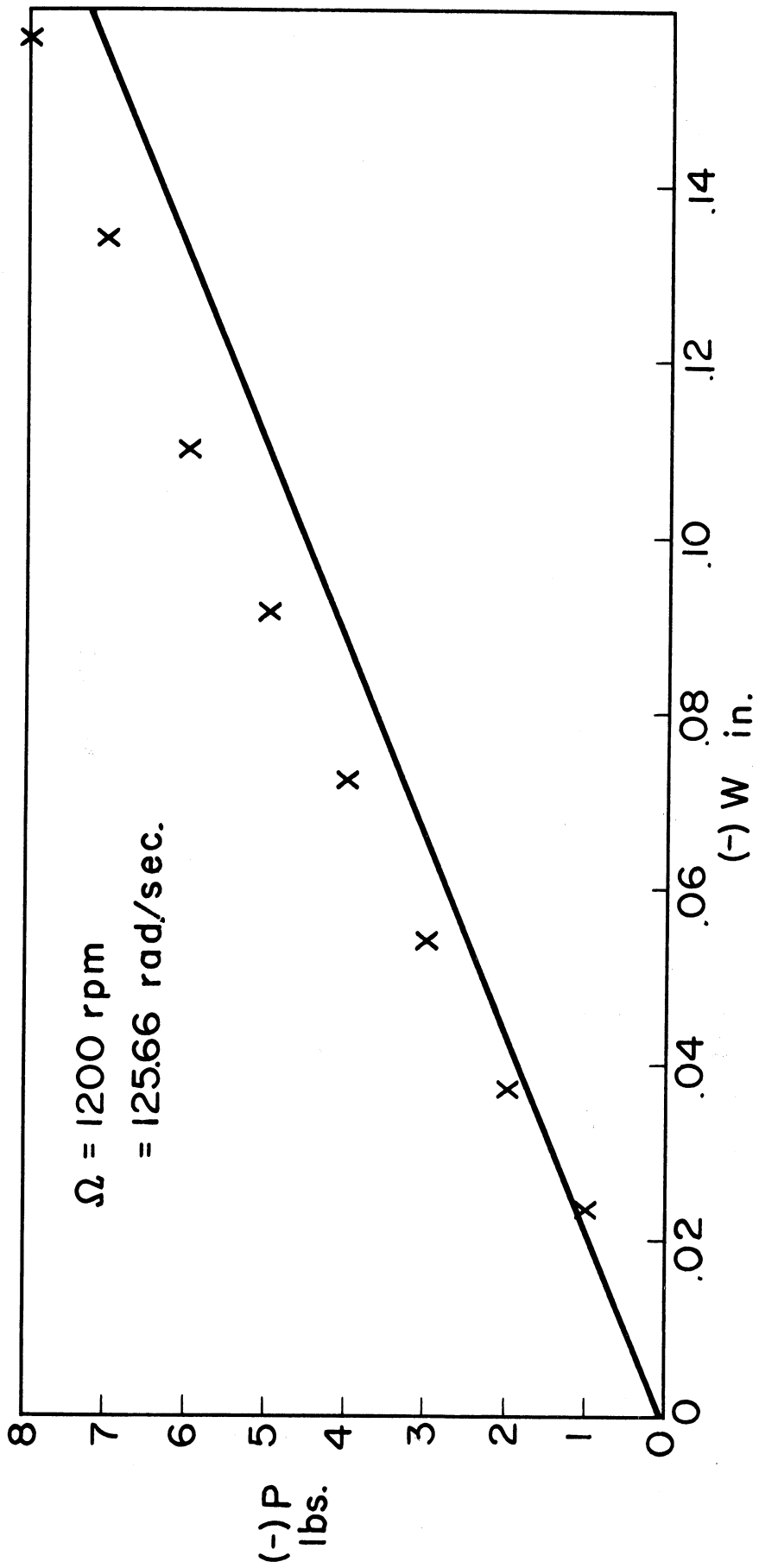


Figure 9. Load vs deflection. Test model 1. $\Omega = 1200 \text{ rpm.}$

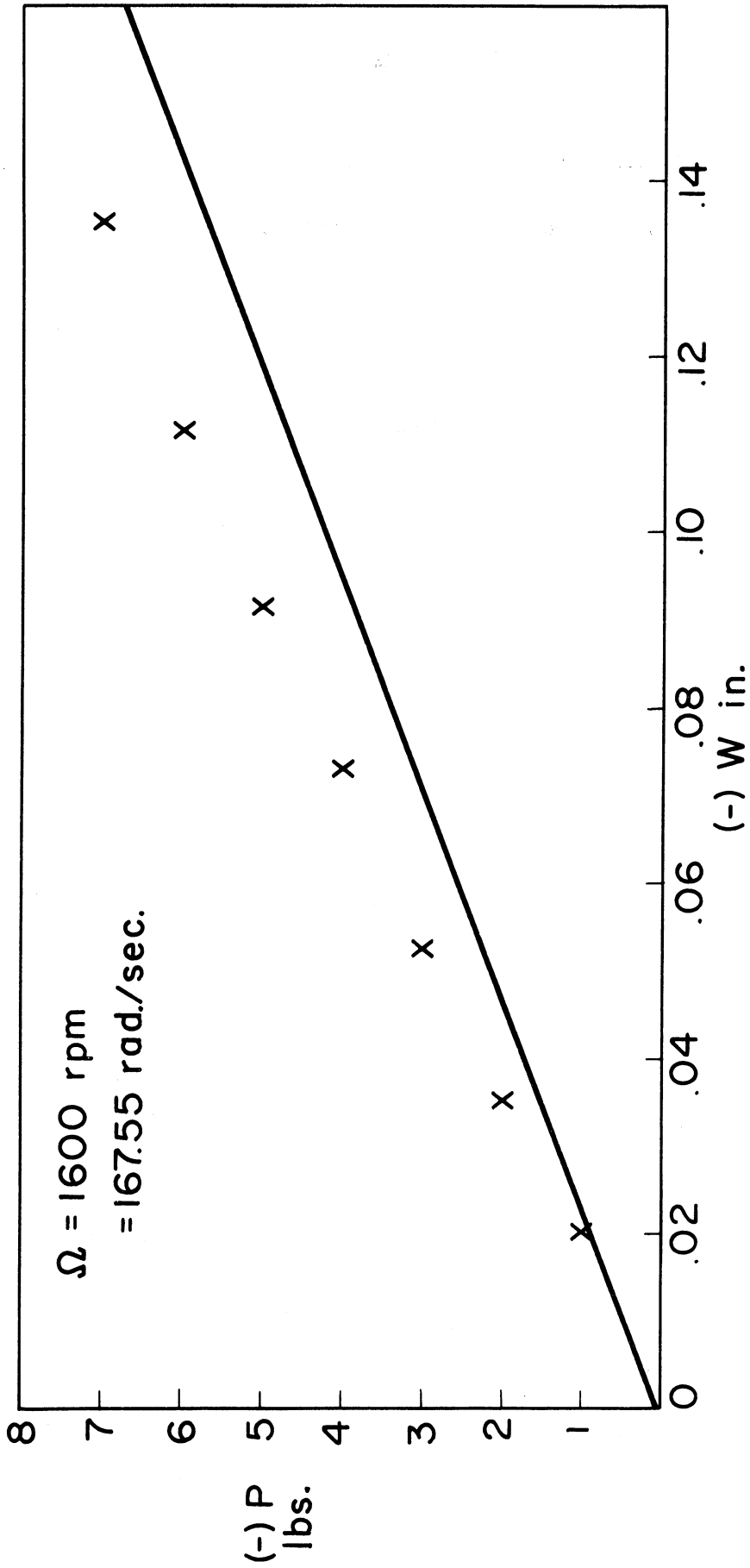


Figure 10. Load vs deflection. Test model 1. $\Omega = 1600 \text{ rpm}$.

ACKNOWLEDGMENT

Most of the experimental data presented here was obtained on equipment designed and constructed by Mr. Robert Cohen.

REFERENCES

1. Clark, S. K., "An Analog for the Static Loading of a Pneumatic Tire", The University of Michigan, Office of Research Administration, Technical Report O2957-19-T, Ann Arbor, Michigan, March 1964.
2. Tielking, J. T., "Plane Vibration Characteristics of a Pneumatic Tire Model". S.A.E. paper.
3. DiTaranto, R. A., and Lessen, M., "Coriolis Acceleration Effect on the Vibration of a Rotating Thin-Walled Circular Cylinder", Journal of Applied Mechanics, December 1964, p. 700.
4. Kenney, J. T., "Steady-State Vibrations of Beam on Elastic Foundation for Moving Load", Journal of Applied Mechanics, December 1954, p. 359.
5. Vlasov, V. Z., "General Theory of Shells and Its Applications in Engineering", NASA Publication, p. 290.

DISTRIBUTION LIST

	No. of Copies
The General Tire and Rubber Company Akron, Ohio	6
The Firestone Tire and Rubber Company Akron, Ohio	6
B. F. Goodrich Tire Company Akron, Ohio	6
Goodyear Tire and Rubber Company Akron, Ohio	6
United States Rubber Company Detroit, Michigan	6
S. S. Attwood	1
R. A. Dodge	1
The University of Michigan ORA File	1
S. K. Clark	1
Project File	10

UNIVERSITY OF MICHIGAN



3 9015 02539 7087